www.nature.com/labinvest

ARTICLE

LncRNA MAPKAPK5_AS1 facilitates cell proliferation in hepatitis B virus -related hepatocellular carcinoma

Lianyuan Tao[1,2,3], Deyu Li[1,2,3]✉, Sengmao Mu[1], Guanjing Tian[1] and Guoyi Yan[1,2,3]

We explored the biological role of long non-coding RNA (lncRNA) MAPKAPK5_AS1 (MAAS) and the mechanism of its differential expression in hepatitis B virus (HBV)-related hepatocellular carcinoma (HCC). Differentially expressed lncRNAs in HBV-related HCC were determined using bioinformatics analysis. Gain-of-function experiments were conducted to evaluate the effect of MAAS on cell proliferation. A xenograft model was established for in vivo experiments. Dual-luciferase reporter assays, chromatin immunoprecipitation, co-immunoprecipitation, and methylated RNA immunoprecipitation were performed to elucidate the underlying molecular mechanisms. MAAS was upregulated in HBV-related HCC cancerous tissues and its high expression was closely related to the poor survival probability of patients. Functional assays revealed that MAAS overexpression facilitated the proliferation of HBV^+HCC cells in vitro and in vivo. Mechanistically, MAAS promoted the MYC proto-oncogene (c-Myc)-induced transcriptional activation of cyclin-dependent kinase 4 (CDK4), CDK6, and S-phase kinase associated protein 2 via stabilizing c-Myc protein, thereby facilitating G1/S transition. The latter contributed to the paradoxical proliferation of HBV^+HCC cells. Although MAAS was upregulated in HBV-related HCC cancerous tissues, it was highly expressed in M2 macrophages, a major phenotype of tumor-associated macrophages in HBV-related HCC, instead of in HBV^+HCC cells. HBeAg, an HBV-associated antigen, further elevated the MAAS level in M2 macrophages by enhancing the methyltransferase-like 3-mediated N6-methyladenosine modification of MAAS. The increased MAAS in the M2 macrophages was then transferred to HBV^+HCC cells through the M2 macrophage-derived exosomes, promoting cell proliferation. Our findings show that HBV^+HCC cell-secreted HBeAg upregulates MAAS expression in M2 macrophages by affecting its m^6A modification. The upregulated MAAS is then transferred to HBV^+HCC cells via exosomes, facilitating the proliferation of HBV^+HCC cells by targeting c-Myc.

Laboratory Investigation (2022) 102:494–504; https://doi.org/10.1038/s41374-022-00731-9

INTRODUCTION

Hepatocellular carcinoma (HCC) is the most frequent type of primary malignant hepatic tumor, accounting for approximately 80% of cases[1]. The primary risk factor for HCC is chronic hepatitis B virus (HBV) infection. Unlike in the uninfected population, the potential risk of HCC is ten times higher in chronic HBV carriers[2]. Despite the availability of an effective vaccine, more than 240 million people worldwide are infected with HBV, and more than half develop to HBV-related HCC[3].

Currently, growing evidence demonstrates that cancer development is extensively regulated by the tumor microenvironment (TME)[4,5]. In many solid tumors, an important component of TME is tumor-associated macrophages (TAMs), which can be classified into M1 and M2 types and are associated with tumor growth, invasion, and immunosuppression[6]. Previous studies have confirmed that TAMs are abundant in HCC, are mainly polarized toward the M2 phenotype, and contribute to the malignant progression of HCC[7]. In HBV-related HCC, the carcinoma tissues of patients also showed a high level of TAMs with a predominately "M2-like" phenotype[8]. M2-like macrophage infiltration has been reported to be involved in persistent HBV infection-induced liver disease and immune impairment in humanized mice[9]. The above mentioned studies suggest the potential role of M2-polarized TAMs in HBV-related HCC development.

Exosomes play a central role in the regulation of cancer development by TAMs[1]. Exosomes are small nanovesicles secreted by several types of cells, including TAMs, and function as intercellular communicators by transferring proteins, RNA, and other molecules from cell to cell[10]. Wu et al.[11] reported that exosomes derived from M2 macrophages transported integrin CD11b/CD18 from TAMs to tumor cells to reinforce the migratory property of HCC cells. Except for protein transportation, TAM-derived exosomes also modulate tumor progression by transferring long non-coding RNAs (lncRNAs) to tumor cells[12]. LncRNAs are a type of non-coding RNA that does not possess a protein-coding ability while being able to regulate gene expressions at epigenetic, transcriptional, and post-transcriptional levels[13]. Upon reaching the tumor cells, lncRNAs participate in tumor progression by modulating tumor-associated gene expression. For example, M2 macrophage-derived exosomal lncRNA SBF2-AS1 facilitates pancreatic cancer cell proliferation by releasing X-linked inhibitor of apoptosis protein expression[14].

[1]Department of Hepatobiliary Surgery, Henan Provincial People's Hospital, People's Hospital of Zhengzhou University, School of Clinical Medicine, Henan University, Zhengzhou, Henan 450003, China. [2]Henan Provincial Key Laboratory of Hepatobiliary and Pancreatic Diseases, Henan Provincial People's Hospital, Zhengzhou, China. [3]Zhengzhou Key Laboratory of Minimally Invasive Treatment for Liver Cancer, Henan Provincial People's Hospital, Zhengzhou, China. ✉email: deyu_li2@126.com

Received: 17 August 2021 Revised: 14 December 2021 Accepted: 27 December 2021
Published online: 9 March 2022

In this study, lncRNA MAPKAPK5_AS1 (MAAS) was found to be upregulated in carcinoma samples of HBV-related HCC and was closely associated with the poor survival probability of patients through bioinformatics analysis. However, MAAS expression level was significantly upregulated in M2 macrophages instead of HBV^{+}HCC cells, suggesting that the high expression of MAAS in HBV-related HCC carcinoma tissues might rely on exosomal transfer from TAMs. This study aimed to explore the role of MAAS in HBV-related HCC and to determine the mechanism of its upregulation in carcinoma samples.

MATERIALS AND METHODS

Bioinformatics analysis

The expression matrices of the transcripts and the corresponding clinicopathological data of the hepatic carcinoma samples were downloaded from The cancer genome atlas (TCGA) datasets. The expression matrices of the mRNA and lncRNA of 106 HBV-related HCC carcinoma samples and seven control samples were extracted using Perl script. The principal component analysis performed on the lncRNA expression matrices using R (R version 3.6.3) showed a marked separation between the hepatic carcinoma samples and control samples (Supplementary Fig. 1A). A differential gene expression analysis of the lncRNA expression matrices between the hepatic carcinoma samples and control samples was performed using the R package DESeq2 (v.1.26.0) with a false discovery ratio below 0.05. A total of 211 differentially expressed lncRNAs (DElncs) were identified in the hepatic carcinoma samples, with 168 lncRNAs upregulated and 43 downregulated (Supplementary Fig. 1B). The DElncs expression matrices of 104 hepatic carcinoma samples with survival time information were selected for univariate COX regression analysis (Wald test, $P < 0.05$), and 20 lncRNAs were screened out (Supplementary Fig. 1C). Then, a multivariate COX regression analysis was performed, and 18 candidate lncRNAs among the 20 lncRNAs were screened out. The variance inflation factor values of the 18 candidate lncRNAs were all less than 10 (Supplementary Fig. 1D). Kaplan–Meier survival analysis was performed on 104 hepatic carcinoma patients divided into the low-expression level and high-expression level groups based on the median expression level of 18 candidate lncRNAs. The results showed a highly significant difference in survival probability between the high and low expression levels of PVT1, PRR7_AS1, TMCC1_AS1, KDM4A_AS1, MAAS, and LINC01011 (Supplementary Fig. 1E). The results of univariate and multivariate Cox regression analyses of the six lncRNAs were consistent.

Sample collection

Thirty-three pairs of HCC carcinoma tissues [HBV(−): $n = 11$, HBV(+): $n = 22$] and paired normal adjacent tissues were collected from HCC patients who underwent curative resection at Henan Provincial People's Hospital. None of the enrolled patients had undergone any radiotherapy or chemotherapy before the operation. This study was approved by the Ethics Committee of Henan Provincial People's Hospital, and all participants signed informed consent form before the study.

Cell culture

Human HBV^{+}HCC cell lines (HepG2.2.15 and PLC5) and HBV^{-}HCC cell lines (HepG2 and HuH-7) used in this study were purchased from Procell (Wuhan, China). These cell lines were cultured in minimum essential medium containing 10% fetal bovine serum and 1% penicillin/streptomycin at 37 °C.

QRT-PCR

Total RNA sample extraction from tissues and cells was performed using TRIzol reagent (Applygen, Beijing, China). Exosomal RNA sample extraction was performed using the Exosomal RNA Isolation Kit (Norgen Biotek, Thorold, Canada). For qRT-PCR, RNA samples were reverse-transcribed using TruScript Reverse Transcriptase and Kits (Norgen Biotek). The quantitative analysis of the mRNA and lncRNA expressions was performed using SYBR Premix Ex Taq II (Takara, Tokyo, Japan). The relative mRNA and lncRNA expressions were calculated using the $2^{-\Delta\Delta CT}$ method. β-actin served as an endogenous control.

Cell transfection

Si-RNA targeting MYC proto-oncogene (c-Myc) and methyltransferase-like 3 (METTL3) were provided by GenScript (Nanjing, China). Si-NC was used as a negative control. For siRNA transfection, Lipofectamine™ RNAiMAX was used (Thermo Fisher, Waltham, MA, USA). Cells at a density of 1×10^6 were treated with siRNA-lipid complex containing 25 pmol si-RNA and later incubated for 6 h. Then, the medium was replaced with a fresh complete medium and incubated for another 42 h.

Lentivirus-MAAS (MAAS OVE) and its negative control NC were constructed by Cyagen (Suzhou, China). For lentivirus infection, the cells were infected with MAAS OVE or NC in the presence of polybrene (8 μg/ml, Merck, Billerica, MA, USA) and later incubated for 24 h. The medium was then replaced with a fresh complete medium and incubated for another 3 days.

Measurements of cell cycle, viability, and proliferation

For the cell cycle analysis, HepG2.2.15 and PLC5 cells subjected to the desired protocols were harvested and fixed. Then, 1×10^6 cells were resuspended in 0.5 ml FxCycle™ PI/RNase Staining Solution (Thermo Fisher) and stained for 20 min at 25°C in the dark. The analysis was conducted using flow cytometry.

For cell viability analysis, HepG2.2.15 and PLC5 cells subjected to the desired protocols were seeded into 96-well plates at a density of 4000 cells/per well. On the following day, the cells were incubated with 10 μl MTT solution (TW Reagent, Shanghai, China) for 3 h, followed by incubation with 100 μl formazan solution (TW Reagent) for another 3 h. The optical density of each well at 570 nm was detected using a microplate reader.

For cell proliferation analysis, HepG2.2.15 and PLC5 cells subjected to the desired protocols were seeded into 12-well plates at a density of 800 cells/per well. After a week of cell culture, the medium was removed, and the cells were fixed and stained with 0.1% crystalline violet solution (Aladdin, Shanghai, China). The number of colonies (>10 cells/colony) was counted.

Generation of M2 macrophages

The human monocyte cell line THP-1 used in this study was provided by Procell. To polarize M0 macrophages, 12-myristate 13-acetate (PMA, 10 ng/ml) was added into the culture medium. After incubation for 24 h, the cells were then incubated with IL-4 (20 ng/ml) and IL-13 (20 ng/ml) for another 72 h to differentiate into M2 macrophages. The phenotypic analysis of M2 macrophages was conducted using a flow cytometer with an anti-human-CD206 antibody (17-2069-42, eBioscience, San Diego, CA, USA).

Extraction of exosomes

Before extraction, M2 macrophages were cultured in the exosome-free medium for 2 days. The culture medium was harvested by centrifuging at $300 \times g$ for 5 min. Then, the culture medium was further centrifuged at $300 \times g$ for 15 min, $2000 \times g$ for 15 min, and $10{,}000 \times g$ for 30 min, and $120{,}000 \times g$ for 70 min (twice). Transmission electron microscopy (TEM) was used to identify the extracted exosomes.

In this study, M2 Exo refers to exosomes derived from M2 macrophages, M2(MAAS) Exo refers to exosomes derived from MASS OVE-infected M2 macrophages, $M2^{HBeAg}$ Exo refers to exosomes derived from HBeAg-induced M2 macrophages, $M2^{HBeAg}$ + si-MAAS Exo refers to exosomes derived from M2 macrophages treated with HBeAg + si-MAAS, $M2^{HBeAg\ +\ si\text{-}NC}$ Exo refers to exosomes derived from M2 macrophages treated with HBeAg + si-NC, and $M2^{HBeAg\ +\ si\text{-}METTL3}$ Exo refers to exosomes derived from M2 macrophages treated with HBeAg + si-METTL3.

Establishment of xenograft model in nude mice

Charles River (Beijing, China) provided the BALB/c nude mice used in this study. For the tumor xenograft models, 1×10^7 HepG2.2.15 cells stably infected with MAAS OVE or NC ($n = 5$ in each group) were subcutaneously injected into mice. The tumor volume of each mouse was measured every 5 days. Xenograft tumors were collected 20 days after injection.

To evaluate the effect of M2-associated exosomes on tumorigenicity, 1×10^7 HepG2.2.15 cells co-cultured with M2 Exo, M2(MAAS)Exo, $M2^{HBeAg}$ Exo, or ($M2^{HBeAg}$ + si-MAAS) Exo were subcutaneously injected into mice ($n = 5$ in each group). Xenograft tumors were collected 20 days after injection, and the tumor volumes were measured. This animal study was approved by the Ethics Committee of Henan Provincial People's Hospital.

Immunohistochemical staining

Xenograft tumors were collected and prepared into 4 μm sections. To evaluate the expression levels of Ki67 and c-Myc in xenograft tumors, immunohistochemical staining was performed, using anti-Ki67 (orb389335, Biorbyt, Cambridge, UK) and anti-c-Myc (orb315624, Biorbyt) antibodies, as previously described[15].

Western blot

Western blot assay was performed as previously reported[16]. The primary antibodies used in this study were as follows: anti-cyclin dependent kinase 4 (CDK4) (ab68266, Abcam, Cambridge, UK), anti-CDK6 (ab241554, Abcam), anti-S-phase kinase associated protein 2 (SKP2) (ab183039, Abcam), anti-c-Myc (orb315624, Biorbyt), and anti- METTL3 antibodies (ab195352, Abcam).

Dual-luciferase reporter assay

A dual-luciferase reporter assay was used to evaluate the effect of MAAS on the promoter activities of CCDK4, CDK6, and SKP2. The promoter sequences of CDK4, CDK6, or SKP2 were subcloned into the pGL3-basic plasmid (Fenghui, Hunan, China). HepG2.2.15 and PLC5 cells were infected with MAAS OVE or NC, followed by the transfection of recombinant vector + pRL-TK vector (Fenghui). The luciferase activity of the recombinant vector was detected using a dual-luciferase reporter assay system (Promega, Madison, WI, USA).

Chromatin immunoprecipitation (CHIP)

The interplay between c-Myc and the promoters of CDK4, CDK6, and SKP2 was evaluated using a CHIP assay. HepG2.2.15 and PLC5 cells infected with MAAS OVE or NC were harvested, treated with 1% formaldehyde, crushed by ultrasound, and then centrifuged. A complex of anti-c-Myc antibody-protein A/G magnetic beads (Thermo Fisher) was added to the supernatant. After 12 h incubation at 4 °C, the endogenous DNA–protein complex was then eluted and subjected to reverse crosslinking. The abundances of CDK4, CDK6, and SKP2 promoters bound with anti-c-Myc antibody were examined using qRT-PCR.

Co-immunoprecipitation (Co-IP)

A co-IP assay was used to explore the effect of MAAS on the ubiquitination of c-Myc. HepG2.2.15 and PLC5 cells were infected with MAAS or NC. Four days later, HepG2.2.15 and PLC5 cells were incubated with 10 μM MG132 for 4 h. Cells were harvested and lysed. A complex of anti-c-Myc-antibody-protein A/G agarose beads was added to the cell lysate. After 12 h of incubation at 4 °C, the protein was eluted and purified. The expression level of ubiquitin in the extracted protein was measured using western blot.

To evaluate the effect of M2-associated exosomes on the ubiquitination of c-Myc, HepG2.2.15 cells were treated with M2 Exo, M2(MAAS) Exo, $M2^{HBeAg}$ Exo, or ($M2^{HBeAg}$ + si-MAAS)Exo, followed by MG132 treatment. The Co-IP assay was then performed as described above.

Methylated RNA immunoprecipitation (Me-RIP)

N6-methyladenosine (m6A) modification was examined using Me-RIP. Anti-m^6A antibody (ab208577, Abcam) was bound with protein A/G magnetic beads (Thermo Fisher) before the assay. Total RNA was extracted from M2 macrophages treated with HBeAg or HBeAg + si-METTL3 using TRIzol reagent, followed by incubation with the antibody-beads complex overnight at 4 °C. The RNA was then eluted and purified. The MAAS level in the extracted RNA was examined using qRT-PCR.

Statistical analyses

Data are presented as means ± standard deviations. SPSS Statistics 20.0 (IBM, Armonk, NY, USA) was used to conduct the statistical analyses. *P*-value was calculated using Student's t-test or a one-way ANOVA. A value of $P < 0.05$ was considered statistically significant.

RESULTS

MAAS is highly expressed in HBV-related HCC carcinoma samples and reinforces the proliferation of HBV^+HCC cells

To explore the novel HBV-related HCC-associated lncRNAs, we analyzed the TCGA database and screened six lncRNAs as risk factors for HBV-related HCC (Fig. 1A and Supplementary Fig. 1). Among these, MAAS was most significantly dysregulated in the HBV-related HCC carcinoma samples we collected (data not shown). Therefore, we selected MAAS for the subsequent investigation. As shown in Fig. 1B, C, MAAS expression was significantly upregulated in the HBV-related HCC carcinoma samples downloaded from the TCGA datasets, and the high MAAS expression level was associated with the low survival probability of HBV-related HCC patients. Ensemble database (www.plants.ensembl.org) revealed that there were several intron splicing modes in the MAAS gene (Supplementary Fig. 2A). The PCR results confirmed that the MAAS in the HBV-related HCC carcinoma samples we collected was MAPKAPK5_AS1-201 (encode ID: ENST00000428207.4) (Supplementary Fig. 2B), which is located on chromosome 12: 111,839,764–111,842,902 and is 2290 bp in length. The MAAS expression was detected in the clinical samples we collected, and the results (Fig. 1D) revealed that MAAS was also distinctly higher in the HBV-related HCC carcinoma tissues than in the paired adjacent normal tissues.

To further determine the biological function of MAAS in HBV-related HCC, HBV^+HCC cell lines HepG2.2.15 and PLC5 were infected with MAAS OVE or NC, followed by cell proliferation and viability measurements. Compared with NC, MAAS OVE significantly reinforced colony formation (Fig. 1E) and cell viability (Fig. 1F) in HepG2.2.15 and PLC5 cells. A xenotransplantation experiment was performed on mice to explore the effect of MAAS on tumor growth in vivo. Compared with mice receiving an injection of NC-HepG2.2.15 cells, mice receiving an injection of MAAS OVE-HepG2.2.15 cells exhibited increased tumor volume (Fig. 1G), and higher Ki67 expression in xenograft tumors (Fig. 1H). These data led to the conclusion that MAAS overexpression facilitates HBV^+HCC cell growth in vitro and in vivo.

The G1/S transition of HBV^+HCC cells enhanced by MAAS overexpression reliees on c-Myc

The effect of MAAS on cell cycle distribution was examined next. As shown in Fig. 2A, MAAS overexpression lessened the G1 phase population while elevating the S phase population in both PLC5 and HepG2.2.15 cells, suggesting that MAAS promoted cell proliferation by facilitating the G1/S transition. Pearson correlation analysis was performed on the expression matrices of the mRNAs and lncRNAs of 106 HBV-related HCC carcinoma samples downloaded from the TCGA datasets. The results showed that there was a positive correlation between MAAS and 12 cell cycle-related genes (Fig. 2B). Using qRT-PCR, the mRNA levels of these 12 genes were examined in HepG2.2.15 and PLC5 cells infected with MAAS OVE or NC, and the results showed that CDK4, CDK6, and SKP2 were commonly upregulated genes in HepG2.2.15 and PLC5 cells infected with MAAS OVE (Fig. 2C, D). Furthermore, western blot analysis demonstrated that MAAS OVE also upregulated the protein levels of CDK4, CDK6, and SKP2 in HepG2.2.15 and PLC5 cells (Fig. 2E).

Given that MAAS overexpression could reinforce both the transcriptions and translations of CDK4, CDK6, and SKP2, and that mRNA transcription occurred prior to protein translation[17], we explored the effect of MAAS on CDK4, CDK6, and SKP2 mRNAs. An RNA polymerase II inhibitor ActD chase assay was conducted to evaluate the effect of MAAS on the mRNA stabilities of CDK4, CDK6, and SKP2. As shown in Fig. 2F, MAAS OVE failed to alter the degradation rates of CDK4, CDK6, and SKP2 mRNAs in HepG2.2.15 and PLC5 cells. A dual-luciferase reporter gene assay was conducted to evaluate the effect of MAAS on the mRNA transcriptions of CDK4, CDK6, and SKP2. As shown in Fig. 2G, the promoter activities of CDK4, CDK6, and SKP2 were significantly increased in HepG2.2.15 and PLC5 cells infected with MAAS OVE compared with the cells infected with NC. These results indicated that MAAS upregulated CDK4, CDK6, and SKP2 expressions by enhancing their transcriptions.

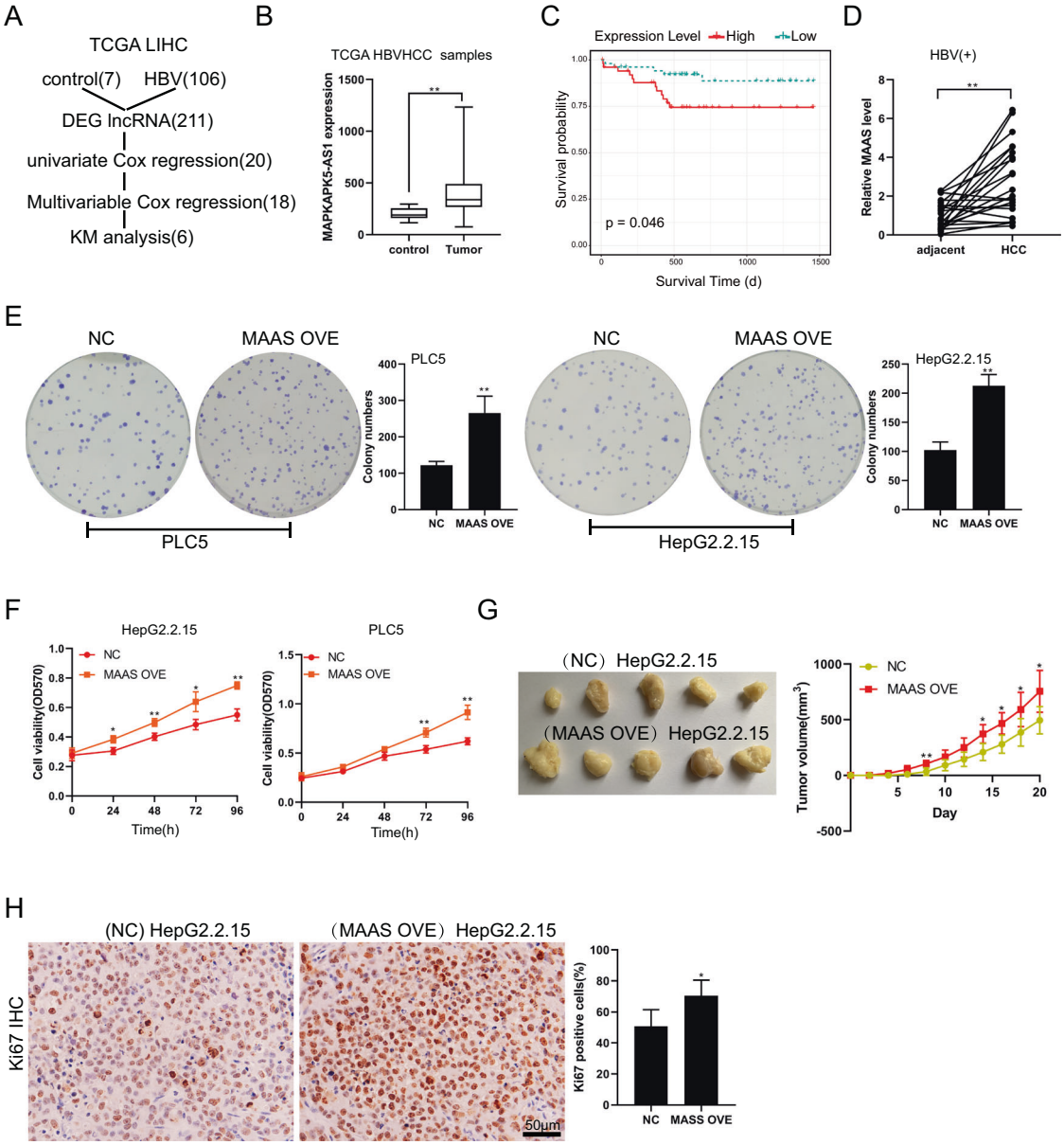

Fig. 1 MAPKAPK5_AS1 (MAAS) is highly expressed in hepatitis B virus (HBV)-related hepatocellular carcinoma (HCC) carcinoma samples and reinforces the growth of HBV$^+$HCC cells. A The protocol of bioinformatics analysis. **B** The MAAS expression in 106 HBV-related HCC carcinoma samples and seven control samples downloaded from the TCGA datasets. $^{**}P < 0.01$. **C** The survival probability of 104 HBV-related HCC patients with high and low expression levels of MAAS (based on the median expression level) was analyzed using Kaplan–Meier survival analysis. **D** Relative MAAS expression levels in 22 pairs of HBV-related HCC carcinoma tissues and normal adjacent tissues were measured using qRT-PCR. $^{**}P < 0.01$. **E**, **F** HBV$^+$HCC cell lines PLC5 and HepG2.2.15 were infected with Lenti-MAAS (MAAS OVE) and its negative control (NC). **E** Cell proliferation was measured using colony formation assay. $^{**}P < 0.01$ vs NC. **F** Cell viability was measured using MTT assay. $^{*}P < 0.05$, $^{**}P < 0.01$ vs NC. **G**, **H** Nude mice were subcutaneously injected with 1×10^7 HepG2.2.15 cells stably infected with MAAS OVE or NC ($n = 5$ in each group), and the xenograft tumors were collected 20 days after injection. **G** Tumor volumes of mice. $^{*}P < 0.05$, $^{**}P < 0.01$ vs NC. **H** Immunohistochemical staining for Ki67 was performed on xenograft tumors (scale bar = 50 μm). $^{*}P < 0.05$ vs NC.

To identify the mechanism through which MAAS modulated CDK4, CDK6, and SKP2 promoter activities, the promoter sequences of these three genes were analyzed. As shown in Fig. 2H, several c-Myc binding sites, including canonical E-box binding sites (cacgtg) and non-canonical binding sites (catgcg and cacgcg)[18], were found in the promoters of CDK4, CDK6, and SKP2. CHIP assay confirmed the combinations of c-Myc and CDK4, CDK6, and SKP2 promoters in HepG2.2.15 and PLC5 cells (Fig. 2H). Therefore, we hypothesized that MAAS enhances CDK4, CDK6, and SKP2 transcriptions by reinforcing the interactions between CDK4, CDK6, and SKP2 promoters and c-Myc. Compared with NC, MAAS OVE significantly increased the enrichment of CDK4, CDK6, and SKP2 promoter fragments in the immunoprecipitated fraction with anti-c-Myc antibody in both HepG2.2.15 and PLC5 cells, which was consistent with our hypothesis (Fig. 2H). The results of cell cycle distribution showed that c-Myc knockdown partly removed the G1/S transition induced by MAAS OVE and arrested more cells in the G1 phase in HepG2.2.15 and PLC5 cells (Fig. 2I). The above results suggested that MAAS overexpression reinforces the G1/S transition of HBV$^+$HCC cells by elevating c-Myc expression.

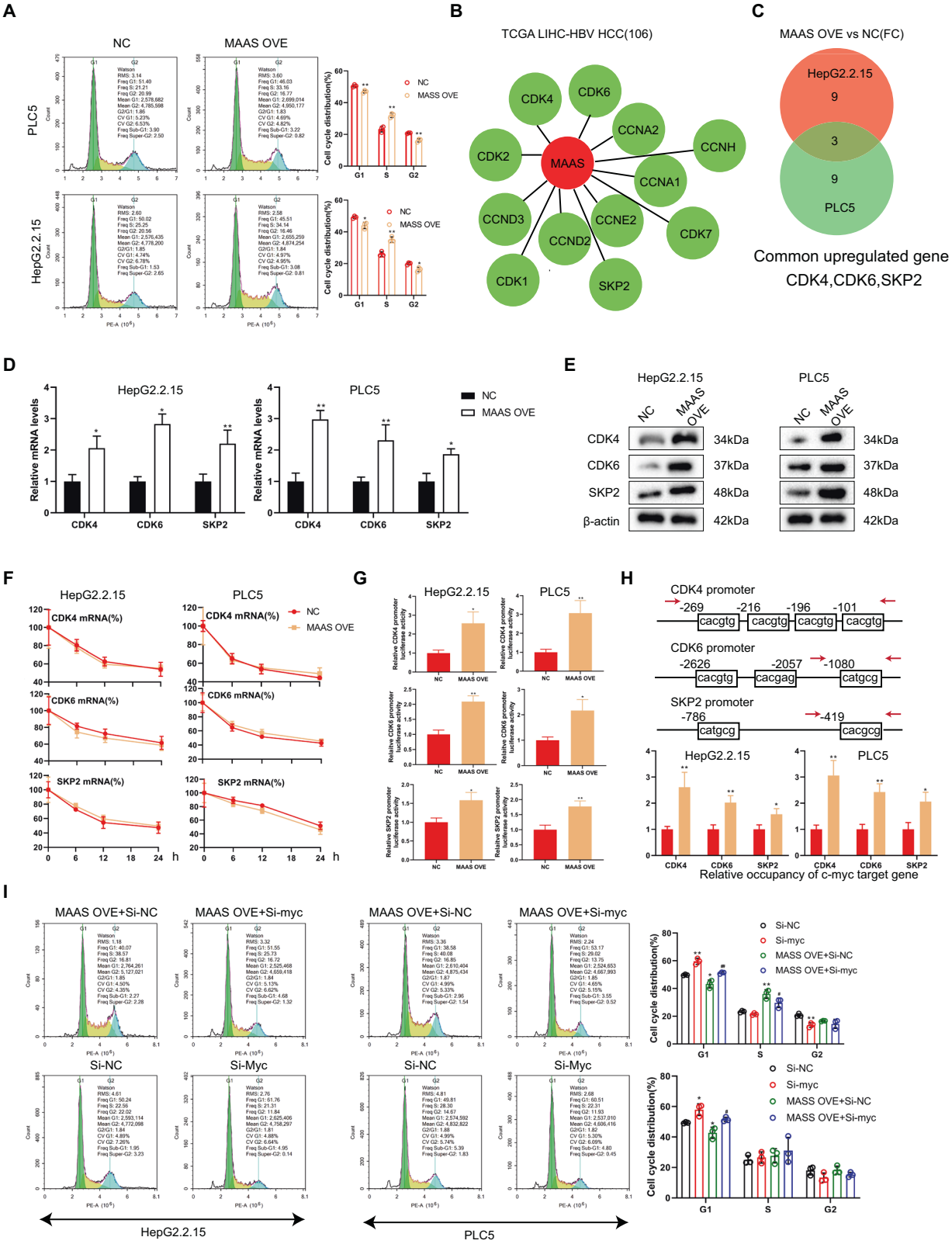

MAAS overexpression enhances the proliferative property of HBV^{+}HCC cells by stabilizing c-Myc protein

The above findings prompted an investigation of the underlying mechanism of the c-Myc upregulation induced by MAAS overexpression. As shown in Fig. 3A, MAAS OVE distinctly increased c-Myc protein levels without altering the mRNA level in HepG2.2.15 and PLC5 cells. Therefore, we hypothesized that MAAS modulates c-Myc expression by affecting its protein degradation. Consistent with our hypothesis, blocking the proteasomal degradation pathway using MG132 (a proteasome

Fig. 2 The G1/S transition of HBV^{+}HCC cells enhanced by MAAS relies on MYC proto-oncogene (c-Myc). A Cell cycle distribution in PLC5 and HepG2.2.15 cells infected with MAAS OVE or NC was examined using flow cytometry. *$P < 0.05$, **$P < 0.01$ vs NC. **B** Pearson correlation analysis revealed that MAAS was positively correlated with cyclin dependent kinase 6 (CDK6), cyclin A2 (CCNA2), cyclin H (CCNH), CCNA1, CDK7, cyclin E2 (CCNE2), S-phase kinase associated protein 2 (SKP2), cyclin D2 (CCND2), CDK1, CCND3, CDK2, CDK4 in 106 HBV-related HCC carcinoma samples downloaded from the TCGA datasets. **C** The mRNA levels of 12 genes in (**B**) were measured using qRT-PCR in PLC5 and HepG2.2.15 cells infected with MAAS OVE or NC (FC = fold change). CDK4, CDK6, and SKP2 are the common upregulated genes and their mRNA levels were shown in (**D**). *$P < 0.05$, **$P < 0.01$ vs NC. **E** The protein levels of CDK4, CDK6, and SKP2 were measured using western blot in PLC5 and HepG2.2.15 cells infected with MAAS OVE or NC. β-actin was used as intern control. **F** PLC5 and HepG2.2.15 cells were infected with NC or MASS OVE, followed by incubation of 5 μg/ml actinomycin D (ActD). The mRNA levels of CDK4, CDK6, and SKP2 were measured using qRT-PCR at indicated times. **G** Promoter activities of CDK4, CDK6, and SKP2 were measured using Dual-luciferase reporter gene assay in PLC5 and HepG2.2.15 cells infected with NC or MASS OVE. *$P < 0.05$, **$P < 0.01$ vs NC. **H** Above: potential c-Myc binding sites in CDK4, CDK6, and SKP2 promoters. Below: The interplays between c-Myc and CDK4, CDK6, and SKP2 promoters were measured using Chromatin Immunoprecipitation (CHIP) assay in PLC5 and HepG2.2.15 cells infected with NC or MASS OVE. *$P < 0.05$, **$P < 0.01$ vs NC. **I** PLC5 and HepG2.2.15 cells were transfected with si-myc, the negative control of si-myc (si-NC), MAAS OVE + si-NC, and MAAS OVE + si-myc, followed by the measurement of cell cycle distribution using flow cytometry. *$P < 0.05$, **$P < 0.01$ vs si-NC, $^{\#}P < 0.05$, $^{\#\#}P < 0.01$ vs MAAS OVE + si-NC.

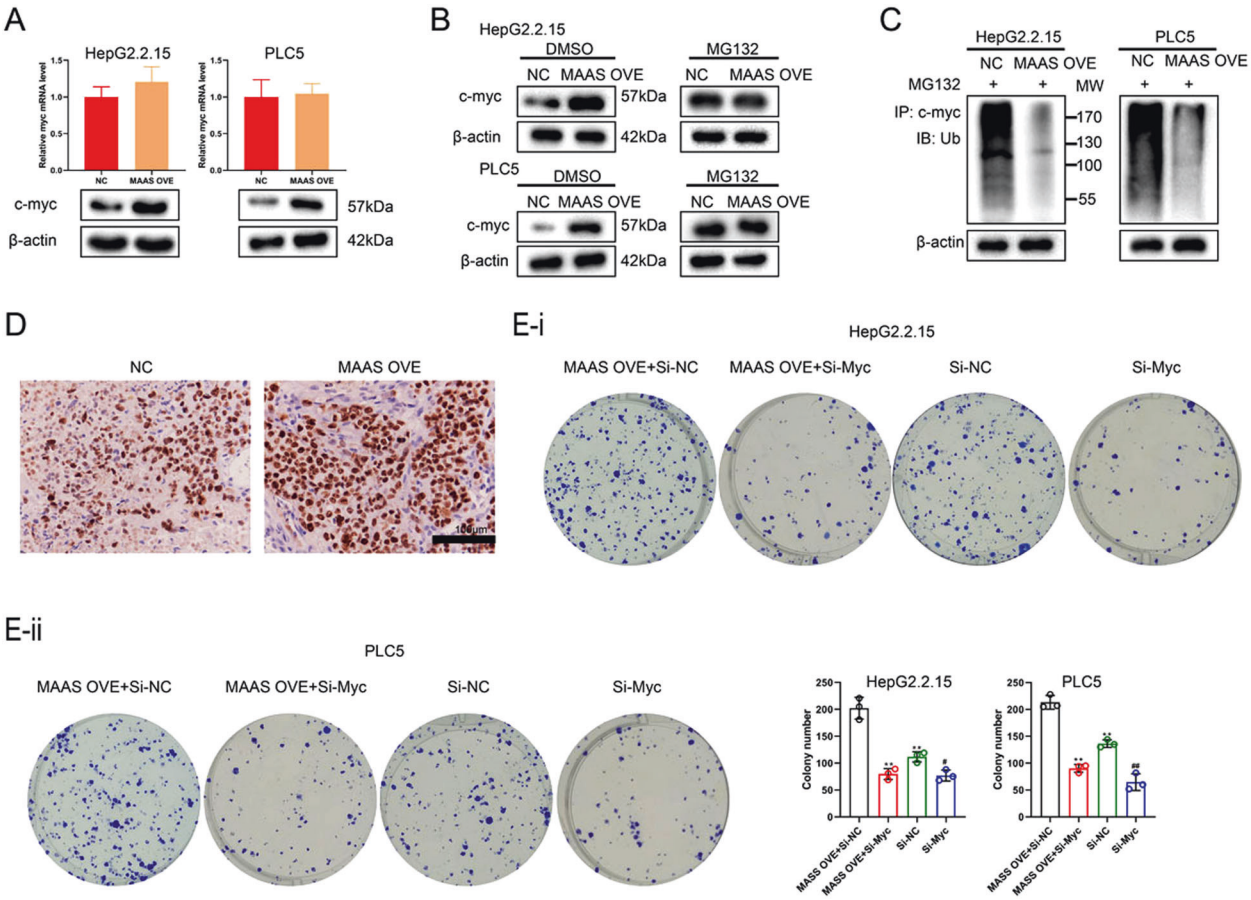

Fig. 3 MAAS enhances the proliferative property of HBV^{+}HCC cells through stabilizing c-Myc protein. A The mRNA and protein levels of c-Myc in PLC5 and HepG2.2.15 cells infected with MAAS OVE or NC. **B** PLC5 and HepG2.2.15 cells were infected with NC or MAAS-OVE, followed by incubation of MG132 (10 μM) or DMSO (solvent control) for 4 h. C-Myc protein levels were measured. **C** The ubiquitination of c-Myc was measured using Co-IP assay in PLC5 and HepG2.2.15 cells treated with MAAS OVE + MG132 or NC + MG132. **D** Immunohistochemical staining for c-Myc was performed on xenograft tumors of mice injected with NC-HepG2.2.15 cells or MAAS OVE-HepG2.2.15 cells (scale bar = 100 μm). **E** PLC5 and HepG2.2.15 cells were transfected with si-myc, si-NC, MAAS OVE + si-NC, and MAAS OVE + si-myc, followed by the measurement of cell proliferation using colony formation assay. **$P < 0.01$ vs MASS OVE + si-NC, $^{\#}P < 0.05$, $^{\#\#}P < 0.01$ vs si-NC.

inhibitor) resulted in the failure of MAAS OVE to upregulate the c-Myc protein level in HepG2.2.15 and PLC5 cells (Fig. 3B). The ubiquitination of c-Myc apparently lessened in HepG2.2.15 and PLC5 cells infected with MAAS OVE compared with the cells infected with NC (Fig. 3C). Based on these findings, we concluded that MAAS upregulated c-Myc expression by weakening its ubiquitin-proteasome degradation pathway. The results of immunohistochemical staining for c-Myc demonstrated that c-Myc expression was noticeably increased in the xenograft tumors of mice injected with MAAS OVE-HepG2.2.15 cells compared with those of mice injected with NC-HepG2.2.15 cells (Fig. 3D). This suggested that MAAS overexpression could also upregulate c-Myc expression in vivo. Subsequently, the role of c-Myc in the proliferation of HBV^{+}HCC cells promoted by MAAS overexpression was evaluated using a colony formation assay. As depicted in Fig. 3E, the interference of c-Myc effectively prevented the increase in colony numbers induced by MASS OVE in HepG2.2.15 and PLC5 cells, suggesting that MASS overexpression enhanced

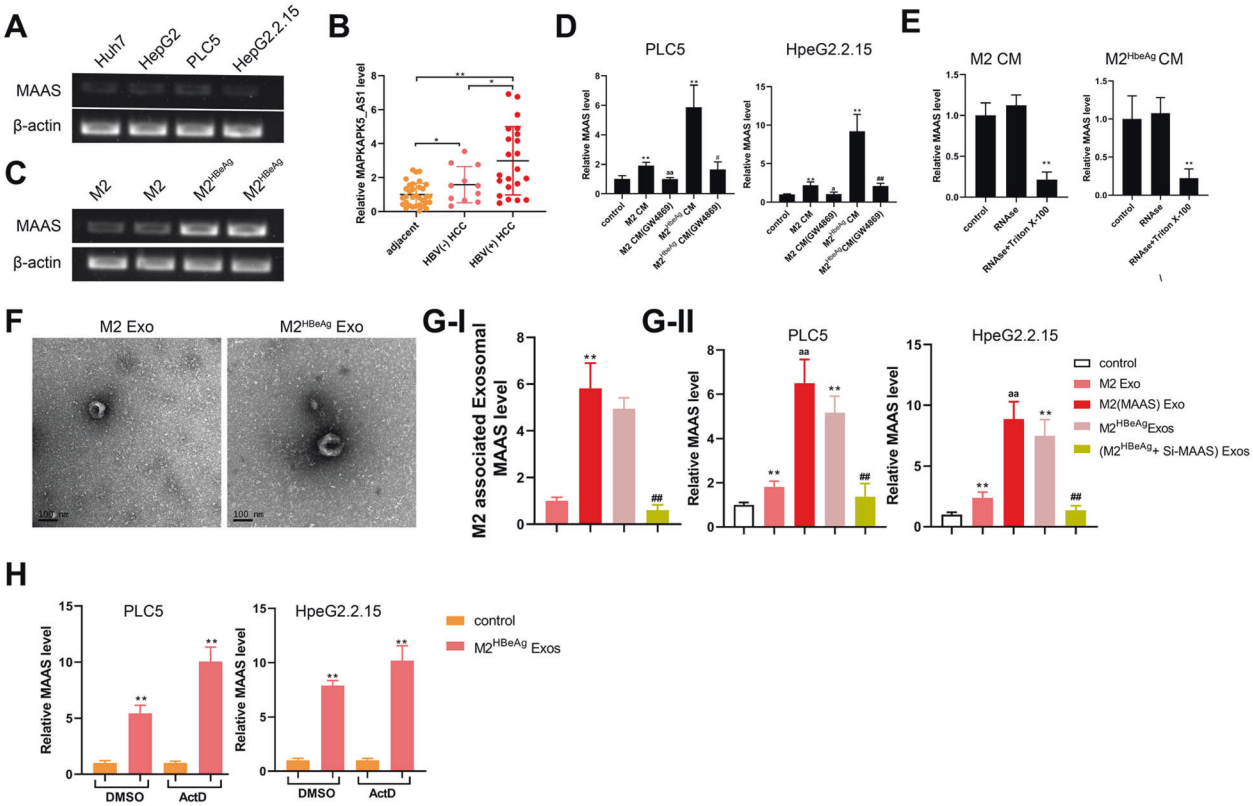

Fig. 4 HBeAg-stimulated M2 macrophages deliver MAAS to HBV$^+$HCC cells via exosomes. A The MAAS expressions in the HBV$^-$HCC cell lines (HepG2 and HuH-7), and HBV$^+$HCC cell lines (PLC5 and HepG2.2.15) were examined using PCR amplification and gel electrophoresis. **B** The MAAS expressions in HBV(-)HCC carcinoma tissues ($n = 11$), HBV(+)HCC carcinoma tissues ($n = 22$), and paired normal adjacent tissues ($n = 33$) were measured by qRT-PCR. **C** The MAAS expression in M2 macrophages generated from THP-1 cells cultured under a normal condition (72 h) or incubated with HBeAg (2 μg/ml, 72 h). **D** The HBV$^+$HCC cell lines were cultured under a normal condition (control) or culture with mediums collected from M2 macrophages (M2 CM), GW4869-treated M2 macrophages [M2 CM (GW4869)], HBeAg-treated M2 macrophages (M2^{HBeAg} CM), and GW4869 + HBeAg-treated M2 macrophages [M2 ^{HBeAg} CM (GW4869)]. 48 h later, the MAAS level in cells was measured. $^{**}P < 0.01$ vs control, $^{a}P < 0.05$, $^{aa}P < 0.01$ vs M2 CM, $^{\#}P < 0.05$, $^{\#\#}P < 0.01$ vs M2^{HBeAg} CM. **E** The MAAS level was measured in the M2 CM and M2^{HBeAg} CM treated with RNAse or RNAse + Triton X-100. $^{**}P < 0.01$ vs CM treated with RNAse. **F** Representative transmission electron microscopy images of exosomes derived from M2 macrophages (M2 Exo) and HBeAg-treated M2 macrophages (M2^{HBeAg} Exo) (Scale bar = 100 nm). **G** I: MAAS level in exosomes derived from M2 macrophages (M2 Exo), MASS OVE-infected M2 macrophages [M2(MAAS) Exo], HBeAg-treated M2 macrophages (M2^{HBeAg} Exo), and M2 macrophages treated with HBeAg + si-MAAS [(M2^{HBeAg} + si-MAAS) Exo]. $^{**}P < 0.01$ vs M2 Exo, $^{\#\#}P < 0.01$ vs M2^{HBeAg} Exo. II: HBV$^+$HCC cell lines were cultured under a normal condition (control) or co-cultured with these four types of Exo and the MAAS level in cells was measured. $^{**}P < 0.01$ vs control M2 macrophages, $^{aa}P < 0.01$ vs M2 macrophages co-cultured with M2 Exo, $^{\#\#}P < 0.01$ vs M2 macrophages co-cultured with M2^{HBeAg} Exo. **H** MAAS levels in HBV$^+$HCC cell lines treated with DMSO, ActD, DMSO + M2^{HBeAg} Exo, or ActD + M2^{HBeAg}. $^{**}P < 0.01$ vs control + DMSO or control + ActD.

the proliferative property of HBV$^+$HCC cells by stabilizing c-Myc protein.

HBeAg-stimulated M2 macrophages deliver MAAS to HBV$^+$HCC cells via exosomes

MAAS expression was low in the HBV$^-$HCC and HBV$^+$HCC cells (Fig. 4A). However, MAAS expression was significantly higher in the HBV(−) and HBV-related HCC carcinoma samples than that in the paired adjacent normal tissues, and it was highest in the HBV-related HCC carcinoma samples (Fig. 4B). Thus, we hypothesized that MAAS might be mainly expressed in other cell types in HCC carcinoma samples and that its expression level is associated with HBV infection, given that TAM is the major component of the tumor stroma and mainly expresses an M2 phenotype in HCC[19]. We examined the MAAS expression level in M2 macrophages generated from THP-1 cells and found that MAAS expression was highly expressed in M2 macrophages compared with HBV$^-$HCC and HBV$^+$HCC cells (Fig. 4A, C). In addition, MAAS expression was increased in M2 macrophages cultured with HepG2.2.15 culture medium (CM) compared with M2 macrophages cultured with HepG2 CM (Supplementary Fig. 3A). In general, aside from HBV-DNA replication, HBV-associated antigens, including HBcAg, HBeAg, and HBsAg, are also rapidly produced after HBV infection[20]. High levels of HBcAg, HBeAg, and HBsAg were detected in HepG2.2.15 cells (data not shown). To determine which antigens contributed to MAAS upregulation in M2 macrophages cultured by HepG2.2.15 CM, M2 macrophages were treated with the three antigens, followed by the measurement of MAAS level. As shown in Supplementary Fig. 3B, HBeAg had the strongest ability to upregulate MAAS level in M2 macrophages compared to other antigens. The results of Fig. 4C also showed that the MAAS level in HBeAg-induced M2 macrophages (M2^{HBeAg}) was higher than that in M2 macrophages cultured under normal conditions. A positive correlation was found between HBeAg levels in the serum and MAAS levels in the carcinoma samples of HBV-related HCC patients (Supplementary Fig. 3C). These findings suggested a hypothesis that HBeAg induces MASS overexpression in TAMs in the HBV-related HCC microenvironment.

Thus, we examined the mechanism of communication between M2 macrophages and HBV$^+$HCC cells using MAAS. As shown in Fig. 4D, the MAAS level was increased in HBV$^+$HCC cells cultured with M2 CM or M2^{HBeAg} CM. However, when M2 or M2^{HBeAg}

macrophages were first treated with GW4869 (an inhibitor of exosome release), followed by the collection of CM, M2 CM (GW4869), or $M2^{HBeAg}$ CM (GW4869), they lost the ability to upregulate MAAS level in HBV^+HCC cells (Fig. 4D). As shown in Fig. 4E, the MAAS levels in M2 CM and $M2^{HBeAg}$ CM did not change with RNase treatment, but they were significantly reduced with RNase + Triton X-100 treatment, indicating that extracellular MAAS was packaged by a membrane instead of being directly released. These findings led to the hypothesis that the transport of MAAS from M2 macrophages to HBV^+HCC cells relies on M2 macrophage-derived exosomes. To verify our hypothesis, exosomes derived from M2 macrophages (M2 Exo), MASS OVE-infected M2 macrophages [M2(MAAS) Exo], $M2^{HBeAg}$ macrophages ($M2^{HBeAg}$ Exo), and M2 macrophages treated with HBeAg+si-MAAS ($M2^{HBeAg}$ + si-MAAS Exo) were collected, respectively. TEM imaging analysis showed that isolated Exos morphologically resembled a cup-shaped structure and were around 100 nm in size (Fig. 4F). Then, HBV^+HCC cells were co-cultured with these four types of exosomes, and the MAAS level in the cells was measured. As shown in Fig. 4G, MAAS levels in M2(MAAS) Exo and $M2^{HBeAg}$ Exo were significantly higher than that in M2 Exo (Fig. 4G-I). Correspondingly, the MAAS level in HBV^+HCC cells co-cultured with M2(MAAS) Exo or $M2^{HBeAg}$ Exo was much higher than that in HBV^+HCC cells co-cultured with M2 Exo (Fig. 4G-II). Similarly, $M2^{HBeAg}$ + si-MAAS Exo loaded less MAAS than $M2^{HBeAg}$ Exo (Fig. 4G-I), resulting in a reduced MAAS level in HBV^+HCC cells co-cultured with $M2^{HBeAg}$ + si-MAAS Exo compared with HBV^+HCC cells co-cultured with $M2^{HBeAg}$ Exo (Fig. 4G-II). Furthermore, the upregulation of MAAS in HBV^+HCC cells co-cultured with $M2^{HBeAg}$ Exo was not affected by ActD (Fig. 4H), excluding the involvement of endogenous induction. Taken together, these results suggested that the oncogenic potential of MAAS might be ascribed to its overexpression in HBeAg-induced TAMs of the HBV-associated HCC microenvironment.

$M2^{HBeAg}$ Exo reinforces the proliferation of HBV^+HCC cells by delivering MAAS

The effect of M2-associated exosomes on the proliferation of HBV^+HCC cells was investigated. As shown in Fig. 5A, the colony numbers were increased in HBV^+HCC cells co-cultured with M2 Exo compared with HBV^+HCC cells cultured under normal conditions. Relative to M2 Exo, $M2^{HBeAg}$ Exo induced more colony numbers in HBV^+HCC cells, while the pro-proliferation ability of M2 Exo enhanced by HBeAg was abrogated by the silencing of MAAS (Fig. 5A). These results suggested $M2^{HBeAg}$ Exo reinforced the proliferation of HBV^+HCC cells by delivering MAAS. Compared with M2 Exo, $M2^{HBeAg}$ Exo upregulated the protein levels of c-Myc, CDK4, CDK6, and SKP2, and decreased the c-Myc ubiquitination in HBV^+HCC cells, whereas all these effects were eliminated when MAAS was absent (Fig. 5B, C). These findings, combined with Figs. 2 and 3, suggest that $M2^{HBeAg}$ Exo delivered MAAS to HBV^+HCC cells, enhanced c-Myc protein stability, and reinforced c-Myc-mediated transcriptions of CDK4, CDK6, and SKP2, thereby facilitating the proliferation of HBV^+HCC cells. In vivo experiments showed that compared with mice injected with M2 Exo-treated HepG2.2.15 cells, mice injected with M2(MAAS) Exo-treated HepG2.2.15 cells and $M2^{HBeAg}$ Exo-treated HepG2.2.15 cells exhibited increased xenograft tumor volumes (Fig. 5D) and elevated c-Myc expressions (Fig. 5E). However, when MAAS was silenced, the promoting effect of $M2^{HBeAg}$ Exo on tumor growth and c-Myc expression was abrogated.

HBeAg stabilizes MAAS by enhancing its m^6A methylation level

We then assessed the mechanism through which HBeAg induced MAAS expression in M2 macrophages. A bioinformatics database m6Avar showed that there were several DRACH and RRACU m^6A sequence motifs in the exon region of MAAS (Fig. 6A). In response to HBeAg induction, the MAAS level in M2 macrophages and M2-Exo was significantly elevated, accompanied by an increased m^6A methylation level in MAAS (Fig. 6B). MAAS degradation was effectively reduced by HBeAg treatment in M2 macrophages (Fig. 6C), given that m^6A methylation regulates multiple RNA processes, such as degradation[21]. We speculated that HBeAg enhanced MAAS stability by promoting its m^6A methylation, thereby upregulating MAAS expression in M2 macrophages. METTL3 is a methyltransferase that mediates m6A methylation[22]. As shown in Fig. 6D, in response to METTL3 knockdown, the MAAS level in M2 macrophages and M2-Exo was reduced, and the m^6A methylation modification level in MAAS was downregulated. METTL3 knockdown abrogated the inhibitory effect of HBeAg on MAAS degradation in M2 macrophages (Fig. 6E). Compared with the exosomes derived from M2 macrophages treated with HBeAg + si-NC ($M2^{HBeAg + si\text{-}NC}$ Exo), exosomes derived from M2 macrophages treated with HBeAg + si-METTL3 ($M2^{HBeAg + si\text{-}METTL3}$ Exo) suppressed the proliferative property of HBV^+HCC cells (Fig. 6F).

DISCUSSION

HBeAg, a secretory protein of HBV, is a well-confirmed risk factor for HCC development[23]. Although a strong relationship between HBeAg and HCC has been reported, the biological role of HBeAg in HBV-related HCC remains to be explored. The results of this study showed that MAAS expression in M2 macrophages was upregulated by HBeAg induction. The highly expressed MAAS was subsequently transferred to HBV^+HCC cells via M2 macrophage-derived exosomes and promoted the proliferation of HBV^+HCC cells by targeting c-Myc. Therefore, upregulation of MAAS induced by HBeAg might be associated with m6A modification.

Recently, increasing evidence has demonstrated the vital role of lncRNAs in the onset and development of cancer[24]. MAAS has been confirmed to be an oncogenic gene. In colorectal cancer (CRC), MAAS modulates the expression of snail homolog 1, a major mediator of epithelial-mesenchymal transformation, by cis-regulating the adjacent gene MK5, thereby enhancing the migratory and invasive potential of CRC cells[25]. In HCC, MAAS is highly expressed in carcinoma tissues, and its high expression is related to the malignant clinical features of HCC patients[26]. In this study, the results of bioinformatics analysis showed that MAAS level was elevated in HBV-related HCC, and that its high expression was correlated with the poor survival probability of patients. Subsequent cell biological analysis demonstrated that MAAS overexpression reinforced the proliferation and viability of HBV^+HCC cells, suggesting that MAAS still functions as an oncogenic gene in HBV-related HCC.

Paradoxical cell proliferation is a hallmark of cancer, and the dysregulation of the cell cycle is its basis. Several cell-cycle therapeutics exhibit promising prospects in combination therapies for cancer[27]. For example, a phase 2 study showed that the combination of CDK4/6 inhibitor palbociclib and letrozole effectively improved progression-free survival in patients with advanced estrogen receptor-positive breast cancer[28]. In the present study, the G1/S transition was enhanced in the MAAS-overexpressed HBV^+HCC cells, accompanied by the upregulation of cell cycle-related genes (CDK4, CDK6, and SKP2). This suggested that MAAS promoted the proliferation of HBV^+HCC cells by regulating cell cycle regulatory factors. Previous studies have confirmed that c-Myc could function as a transcription factor of CDK4 and CDK6 and upregulate their expressions[29,30]. Consistent with previous reports, the results of the CHIP and dual-luciferase reporter gene assays confirmed that c-Myc enhanced the promoter activities of CDK4 and CDK6 by binding directly to their promoter, and that these combinations were further reinforced by MAAS overexpression. We also confirmed the transcriptional activation of SKP2 induced by c-Myc; similarly, this transcriptional activation was enhanced by MAAS overexpression. More

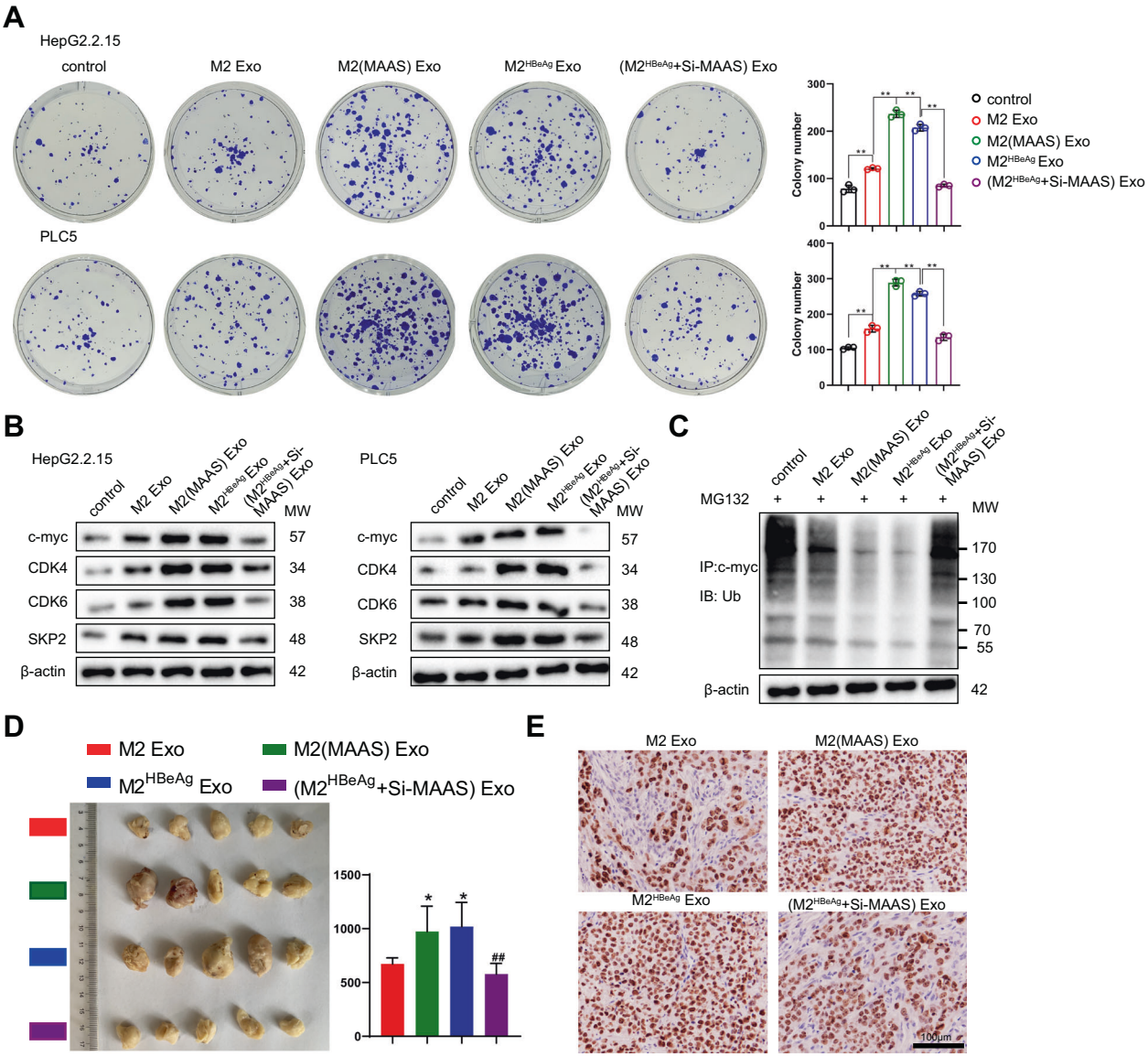

Fig. 5 M2^{HBeAg} Exo reinforces proliferation of HBV^{+}HCC cells by delivering MAAS. A–C PLC5 and HepG2.2.15 cells were cultured under a normal condition (control) or co-cultured with M2 Exo, M2(MAAS) Exo, M2^{HBeAg} Exo, or (M2^{HBeAg} + si-MAAS) Exo. **A** Cell proliferation was measured using colony formation assay. $^{**}P < 0.01$. **B** Protein levels of c-Myc, CDK4, CDK6, and SKP2 were measured using western blot. **C** The ubiquitination of c-Myc was measured using the Co-IP assay. **D, E** Nude mice were subcutaneously injected with 1×10^7 HepG2.2.15 cells co-cultured with M2 Exo, M2(MAAS) Exo, M2^{HBeAg} Exo, or (M2^{HBeAg} + si-MAAS) Exo ($n = 5$ in each group). Twenty days after injection, all mice were euthanatized and xenograft tumors were collected. **D** The tumor volumes of mice. $^{*}P < 0.05$ vs M2 Exo, $^{\#\#}P <$ M2^{HBeAg} Exo. **E** Immunohistochemical staining for c-Myc was performed on xenograft tumors (scale bar = 100 μm).

importantly, c-Myc knockdown effectively retarded the G1/S transition in HBV^{+}HCC cells, whereas this trend was not reversed by MAAS overexpression, indicating that the regulatory effect of MAAS on cell cycle distribution relied on c-Myc. Our study is not the first to report on the role of c-Myc in HBV-related HCC. According to Tsuchiya et al., c-Myc activated the promoter of unconventional prefoldin RNA polymerase II subunit five interactor, an oncogenic driver in HBV-related HCC, by interacting with its E-box in the promoter region[31]. One of the major ways of controlling c-Myc level in cells is reportedly through the ubiquitin-proteasome degradation pathway[32]. In the current study, the combination of ubiquitin and c-Myc was reduced upon MAAS overexpression in HBV^{+}HCC cells, suggesting that MAAS increased C-Myc expression by suppressing its ubiquitin-proteasome degradation pathway. Consistent with our study, several researchers have reported that lncRNAs regulate a specific protein expression by affecting the targeted degradation of the ubiquitin-proteasome system[33,34].

Faure-Dupuy et al.[35]. showed that HBV regulated the function of hepatic macrophages in facilitating the establishment and possible maintenance of infection. Wang et al.[36]. reported that HBeAg elevated microRNA-155 expression in macrophages through the nuclear transcription factor-kappa B signal pathway, thereby increasing the inflammatory cytokine-secreted by macrophages. In this study, we found that MAAS was enriched in M2 macrophages instead of HBV^{+}HCC cells, and that HBeAg induction further upregulated MAAS expression level in M2 macrophages. The increased MAAS was then transferred to HBV^{+}HCC cells through M2 macrophage-derived exosomes, facilitating cell proliferation.

We subsequently focused on the mechanism through which HBeAg modulated MAAS expression. m^{6}A is the most prevalent mRNA modification in eukaryotic cells and is regulated by m^{6}A

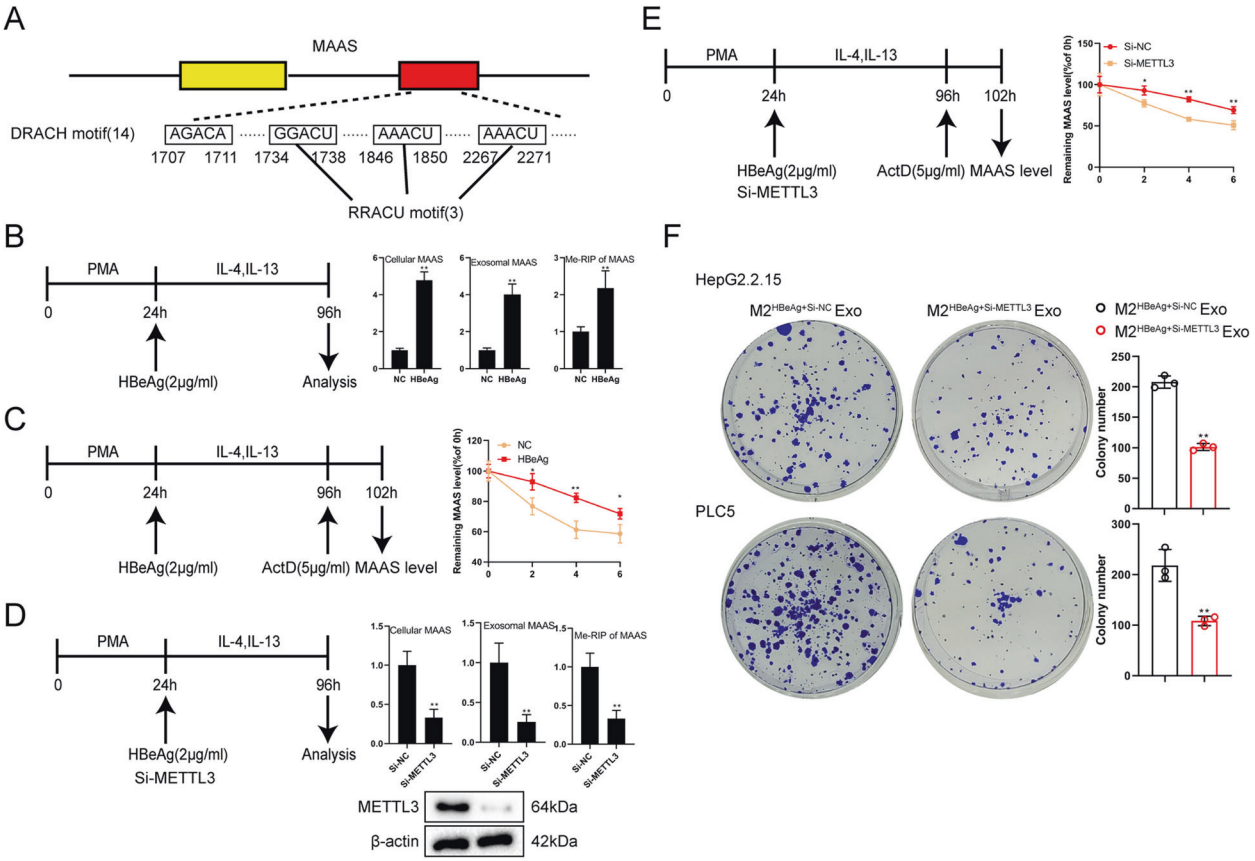

Fig. 6 HBeAg stabilizes MAAS by enhancing its m^{6}A methylation level. A DRACH and RRACU m^{6}A sequence motifs in the exon region of MAAS. **B** During the differentiation of M2 macrophages, HBeAg (2 μg/ml) was added into the culture medium. The MAAS level in M2 macrophages and M2 Exo were measured using qRT-PCR. Methylated RNA immunoprecipitation (Me-RIP) assay was performed to measure the enrichment of m6A-modified MAAS. $^{**}P < 0.01$ vs NC. **C** During the differentiation of M2 macrophages, HBeAg (2 μg/ml) and ActD (2 μg/ml) were added into the culture medium. The MMAS mRNA levels were measured using qRT-PCR at indicated times. $^{*}P < 0.05$, $^{**}P < 0.01$ vs NC. **D** During the differentiation of M2 macrophages, HBeAg (2 μg/ml) and si-methyltransferase-like 3 (si-METTL3)/its negative control (si-NC) were added into the culture medium. The MAAS level in M2 macrophages and M2 Exo were measured using qRT-PCR. The enrichment of m6A-modified MAAS was measured using Me-RIP assay. METTL3 protein level was measured using western blot. $^{**}P < 0.01$ vs si-NC. **E** During the differentiation of M2 macrophages, HBeAg (2 μg/ml), si-METTL3/si-NC, and ActD (2 μg/ml) was added into the culture medium. The MMAS mRNA levels were measured using qRT-PCR at indicated times. $^{*}P < 0.05$, $^{**}P < 0.01$ vs si-METTL3. **F** HBV$^+$HCC cell lines were co-cultured with exosomes derived from M2 macrophages treated with HBeAg + si-NC (M2$^{\text{HBeAg + si-NC}}$ Exo) or M2 macrophages treated with HBeAg + si-METTL3 (M2$^{\text{HBeAg + si-METTL3}}$ Exo). Cell proliferation was measured using colony formation assay. $^{**}P < 0.01$ vs M2$^{\text{HBeAg + si-NC}}$ Exo.

methyltransferases, demethylases, and m^{6}A-binding proteins[37]. Kim et al.[38]. reported that HBV contributed to HCC progression by affecting the m^{6}A modification of phosphatase and tensin homolog, which are well-recognized anti-oncogenes. In addition to mRNA, the expression of lncRNAs is regulated by m^{6}A modification. In HCC cell lines, the stability of LINC00958 was promoted by METTL3-mediated m^{6}A modification, resulting in an increased expression level of LINC00958[39]. However, whether HBV can modulate the m^{6}A modification of lncRNAs has yet to be elucidated. In the present study, we found that HBeAg induced m^{6}A methylation in MAAS in M2 macrophages and reduced its degradation, whereas these effects were abrogated upon METTL3 knockdown, suggesting that the upregulation of MAAS induced by HBeAg was attributed to the METTL3-mediated m^{6}A modification.

In summary, this study showed that HBV$^+$HCC cells-secreted HBeAg upregulated MAAS expression in M2 macrophages by affecting its m^{6}A modification. The upregulated MAAS is transferred to HBV$^+$HCC cells via exosomes, facilitating the proliferation of HBV$^+$HCC cells. Our study highlights the novel role of MAAS in modulating cell proliferation in HBV-related HCC and elucidates the mechanism of HBeAg-induced HBV-related HCC development. It is important to note that primary cells were not used in this study. Due to the limited source of fresh human tissues and the long culture cycle for primary cells[40], the success of primary cell culture is difficult. In addition, HBV-related HCC studied in this paper required the addition of HBV infection of primary cells, which made the subsequent experiment more difficult. We will attempt to verify the main point of this study in primary cells in the future.

DATA AVAILABILITY

All data generated during this study are available within the article.

REFERENCES

1. Guo, W., Li, Y., Pang, W. & Shen, H. Exosomes: a potential therapeutic tool targeting communications between tumor cells and macrophages. *Mol. Ther.* **28**, 1953–1964 (2020).
2. El-Serag, H. B. Epidemiology of viral hepatitis and hepatocellular carcinoma. *Gastroenterology*. **142**, 1264–1273.e1261 (2012).
3. Morikawa, K. et al. Hepatitis B: progress in understanding chronicity, the innate immune response, and cccDNA protection. *Ann. Transl. Med*. **4**, 337 (2016).
4. Wang, J. J., Lei, K. F. & Han, F. Tumor microenvironment: recent advances in various cancer treatments. *Eur. Rev. Med. Pharmacol. Sci.* **22**, 3855–3864 (2018).
5. Geng, W.-R. Radiotherapy alters the polarization of tumor-associated macrophage to suppress lung cancer progression via up-regulation of lincRNA-p21. *Clin. Surg. Res. Commun.* **1**, 01–07 (2019).

6. Chen, Y. et al. Tumor-associated macrophages: an accomplice in solid tumor progression. *J. Biomed. Sci*. **26**, 78 (2019).
7. Huang, Y. et al. The role of tumor associated macrophages in hepatocellular carcinoma. *J. Cancer*. **12**, 1284–1294 (2021).
8. Luo, H. L. et al. Downregulation of macrophage-derived T-UCR uc.306 associates with poor prognosis in hepatocellular carcinoma. *Cell Physiol. Biochem*. **42**, 1526–1539 (2017).
9. Bility, M. T. et al. Hepatitis B virus infection and immunopathogenesis in a humanized mouse model: induction of human-specific liver fibrosis and M2-like macrophages. *PLoS Pathog*. **10**, e1004032 (2014).
10. Aslan, C. et al. Tumor-derived exosomes: Implication in angiogenesis and anti-angiogenesis cancer therapy. *J. Cell Physiol*. **234**, 16885–16903 (2019).
11. Wu, J. et al. M2 macrophage-derived exosomes facilitate HCC metastasis by transferring α(M) β(2) integrin to tumor cells. *Hepatology*. **73**, 1365–1380 (2021).
12. Chen, F. et al. The functional roles of exosomes-derived long non-coding RNA in human cancer. *Cancer Biol. Ther*. **20**, 583–592 (2019).
13. Zhu, J., Fu, H., Wu, Y. & Zheng, X. Function of lncRNAs and approaches to lncRNA-protein interactions. *Sci. China Life Sci*. **56**, 876–885 (2013).
14. Yin, Z. et al. Down-regulated lncRNA SBF2-AS1 in M2 macrophage-derived exosomes elevates miR-122-5p to restrict XIAP, thereby limiting pancreatic cancer development. *J. Cell Mol. Med*. **24**, 5028–5038 (2020).
15. Parihar, M. et al. Sex-dependent lifespan extension of Apc (Min/+) FAP mice by chronic mTOR inhibition. *Aging Pathobiol Ther*. **2**, 187–194 (2020).
16. Wu, Z. et al. MiR-4310 induced by SP1 targets PTEN to promote glioma progression. *Cancer Cell Int*. **20**, 567 (2020).
17. Rinn, J. L. & Chang, H. Y. Genome regulation by long noncoding RNAs. *Annu Rev Biochem*. **81**, 145–166 (2012).
18. Kim, J., Lee, J. H. & Iyer, V. R. Global identification of Myc target genes reveals its direct role in mitochondrial biogenesis and its E-box usage in vivo. *PLoS ONE* **3**, e1798 (2008).
19. Zhang, Q. et al. Fatty acid oxidation contributes to IL-1β secretion in M2 macrophages and promotes macrophage-mediated tumor cell migration. *Mol. Immunol*. **94**, 27–35 (2018).
20. Liu, Y. et al. Long non-coding RNA HULC activates HBV by modulating HBx/STAT3/miR-539/APOBEC3B signaling in HBV-related hepatocellular carcinoma. *Cancer Lett*. **454**, 158–170 (2019).
21. Chen, X. Y., Zhang, J. & Zhu, J. S. The role of m(6)A RNA methylation in human cancer. *Mol. Cancer*. **18**, 103 (2019).
22. Zeng, C., Huang, W., Li, Y. & Weng, H. Roles of METTL3 in cancer: mechanisms and therapeutic targeting. *J. Hematol Oncol*. **13**, 117 (2020).
23. Yang, H. I. et al. Hepatitis B e antigen and the risk of hepatocellular carcinoma. *N. Engl. J. Med*. **347**, 168–174 (2002).
24. Li, P. et al. LINC00271 inhibits epithelial-mesenchymal transition of papillary thyroid cancer cells by downregulating trefoil factor 3 expression. *Aging Pathobiol. Ther*. **2**, 78–85 (2020).
25. Yang, T. et al. Long noncoding RNA MAPKAPK5-AS1 promotes colorectal cancer progression by cis-regulating the nearby gene MK5 and acting as a let-7f-1-3p sponge. *J. Exp. Clin. Cancer Res*. **39**, 139 (2020).
26. Wang, L. et al. Long non-coding RNA MAPKAPK5-AS1/PLAGL2/HIF-1α signaling loop promotes hepatocellular carcinoma progression. *J. Exp. Clin. Cancer Res*. **40**, 72 (2021).
27. Ingham, M. & Schwartz, G. K. Cell-cycle therapeutics come of age. *J. Clin. Oncol*. **35**, 2949–2959 (2017).
28. Finn, R. S. et al. The cyclin-dependent kinase 4/6 inhibitor palbociclib in combination with letrozole versus letrozole alone as first-line treatment of oestrogen receptor-positive, HER2-negative, advanced breast cancer (PALOMA-1/TRIO-18): a randomised phase 2 study. *Lancet Oncol*. **16**, 25–35 (2015).
29. Ouyang, Q. et al. Neurotensin signaling stimulates glioblastoma cell proliferation by upregulating c-Myc and inhibiting miR-29b-1 and miR-129-3p. *Neuro. Oncol*. **18**, 216–226 (2016).
30. Luo, W. et al. c-Myc inhibits myoblast differentiation and promotes myoblast proliferation and muscle fibre hypertrophy by regulating the expression of its target genes, miRNAs and lincRNAs. *Cell Death Differ*. **26**, 426–442 (2019).
31. Tsuchiya, H. et al. HBx and c-MYC Cooperate to Induce URI1 Expression in HBV-Related Hepatocellular Carcinoma. *Int. J. Mol. Sci*. **20**, 5714 (2019).
32. Farrell, A. S. & Sears, R. C. MYC degradation. *Cold Spring Harb Perspect Med*. **4**, a014365 (2014).
33. Ni, W. et al. A novel lncRNA uc.134 represses hepatocellular carcinoma progression by inhibiting CUL4A-mediated ubiquitination of LATS1. *J. Hematol. Oncol*. **10**, 91 (2017).
34. Li, Z. et al. The degradation of EZH2 mediated by lncRNA ANCR attenuated the invasion and metastasis of breast cancer. *Cell Death Differ*. **24**, 59–71 (2017).
35. Faure-Dupuy, S. et al. Hepatitis B virus-induced modulation of liver macrophage function promotes hepatocyte infection. *J. Hepatol*. **71**, 1086–1098 (2019).
36. Wang, W. et al. HBeAg induces the expression of macrophage miR-155 to accelerate liver injury via promoting production of inflammatory cytokines. *Cell Mol. Life Sci*. **75**, 2627–2641 (2018).
37. Wu, F. et al. Association of N6-methyladenosine with viruses and related diseases. *Virol J*. **16**, 133 (2019).
38. Kim, G. W. et al. HBV-induced increased n6 methyladenosine modification of PTEN RNA affects innate immunity and contributes to HCC. *Hepatology*. **73**, 533–547 (2021).
39. Zuo, X. et al. M6A-mediated upregulation of LINC00958 increases lipogenesis and acts as a nanotherapeutic target in hepatocellular carcinoma. *J. Hematol. Oncol*. **13**, 5 (2020).
40. Schulze-Bergkamen, H. et al. Primary human hepatocytes-a valuable tool for investigation of apoptosis and hepatitis B virus infection. *J. Hepatol*. **38**, 736–744 (2003).

AUTHOR CONTRIBUTIONS

Participated in research design: LT and DL. Conducted experiments: LT, SM, and GT. Methodology: GT and GY. Performed data analysis: LT, SM, and GY. Wrote or contributed to the writing of the manuscript: LT and DL. All authors have read and agreed to the published version of the manuscript.

FUNDING

This study was supported by grants from the Joint Project of Medical Science and Technology Research Program of Henan Province (LHGJ20190577), Medical Science and Technology Research Plan of Henan Province, Project Co-built by Provincial Department (SB20190319), and Henan Province Health Science and Technology Innovation Excellent Young Talents Training Project (No. YXKC2020044).

COMPETING INTERESTS

The authors declare no competing interests.

ETHICS APPROVAL

This study was approved by the Ethics Committee of the Henan Provincial People's Hospital.

CONSENT TO PARTICIPATE

All the participants signed informed consents before the study.

ADDITIONAL INFORMATION

Supplementary information The online version contains supplementary material available at https://doi.org/10.1038/s41374-022-00731-9.

Correspondence and requests for materials should be addressed to Deyu Li.